Temperature Dependence of Hydrogen Bonding and Freezing Behavior of Water in Reverse Micelles

Nathaniel V. Nucci* and Jane M. Vanderkooi

Department of Biochemistry and Biophysics, University of Pennsylvania, Philadelphia, Pennsylvania 19104

Received: March 2, 2005; In Final Form: June 14, 2005

The mid-infrared spectra of H_2O and D_2O confined in Aerosol OT (AOT) reverse micelles at various water/surfactant molar ratios (w_o) were measured. Previous descriptions of reverse micellar (RM) water have identified three different hydrogen bonding populations in the water pool. (Onori, G.; Santucci, A. *J. Phys. Chem.* **1993**, *97*, 5430−5434.) Fitting of the O−H and O−D stretching vibrational modes to Gaussian components corresponding to these three H-bonding populations was used to determine the temperature dependence of the hydrogen bonding populations and to observe the freezing behavior of the encapsulated water pool. The H-bond network behavior of the RM water pool exhibits a strong dependence on w_o and does not approximate that of bulk water until $w_o = 40$. The freezing temperature of RM water was w_o-independent. The infrared spectra of frozen RM samples has also led us to suggest a mechanism for the low-temperature phase transition behavior of AOT reverse micelles, a subject of interest for cryoenzymology and low-temperature structural biology.

Introduction

Reverse micelles (RMs), or water-in-oil microemulsions, are inverted micelles that spontaneously organize from a mixture of water, amphiphile, and nonpolar solvent, allowing encapsulation of small water pools in a low viscosity, nonpolar solvent.[1,2] They have been widely used to mimic membrane systems and to study biological molecules in a secluded space with sequestered solvent.[1,2] This organized medium serves as an excellent model for the confined conditions of biological molecules in living systems as well as for analysis of nanoscale water behavior. Recently, RMs have been used to investigate the water H-bond network using both ultrafast vibrational spectroscopic techniques and quasi-elastic neutron scattering.[3−5] Bis(2-ethylhexyl) sulfosuccinate (AOT) is the most common surfactant used in RM studies, and the properties of AOT RMs have been extensively explored.[2] Much of the characterization of AOT RM systems has focused on the encapsulated RM water pool. Though many of the properties of RM water are well understood, an in-depth examination of the H-bonding properties of reverse micellar water populations has not yet been reported.

The most important property of reverse micellar systems is their ability to mimic biological conditions by simulating the solvation properties that exist in biological systems. Previous examinations of RM water have demonstrated that as the water/surfactant molar ratio (w_o) increases, the RM water pool grows in diameter, gradually approaching the behavior of bulk water with respect to many properties.[2] Most characteristics of the RM water pool have been shown to closely approximate those of bulk water at all $w_o \geq 20$.[2] It is generally accepted that the RM water pool at any $w_o \geq 20$ approximates bulk water properties.

Infrared spectroscopy is an excellent tool for examining the H-bond arrangement of water populations and has been used to characterize RM water under many conditions.[2,6−18] The water pool of reverse micelles is viewed as a two-population system with a bound water layer associated with the surfactant surface and a core of bulklike water.[6,8,9] Previous analyses of the O−H stretching absorption of RM water have demonstrated that fitting this absorption to a series of three Gaussian functions allows quantitative observation of the different water populations within the reverse micelle.[8,14] The procedure of Onori and Santucci has been used by several groups to analyze RM water structure under many conditions.[7,11,12,14−16] This procedure involves fitting the O−H stretching vibration to three Gaussian components centered at 3603 ± 6, 3465 ± 5, and 3330 ± 30 cm^{-1}.[14] These starting frequencies are based on the populations characterized in bulk water, but in the RM water pool they correspond to the surfactant-bound water layer (high frequency) and two H-bond configurations of the bulklike water core.[14] These three populations are discussed in detail by Brubach, et al.[11] They describe the high-frequency component as corresponding to the bound water, which is made up of water molecules either solvating the surfactant headgroups (highly strained H-bonds) or trapped in the micellar interface (few or no H-bonds). The two lower frequency components are attributed to bulklike water with moderately strained H-bond angles (intermediate frequency) and unstrained H-bond angles (low frequency).[11] This decomposition analysis has been used recently to monitor RM water structure during a chemical process.[15] By combining this procedure with temperature-dependent IR, it is possible to examine the response of the RM water network to temperature perturbation.

The temperature dependence of fundamental infrared absorbances has been shown to be an excellent means of measuring hydrogen bonding.[19,20] Since H-bonding strength increases as temperature is lowered, it follows that stretching modes of groups H-bonded to water shift to lower frequency with decreasing temperature, while bending modes of these groups shift to higher frequency. Modes that are not affected by H-bonding with water are temperature independent, as we have previously demonstrated for tyrosine.[21,22] The merits and applications of this technique for biomolecule−water interac-

* Corresponding author. E-mail: nvnucci@mail.med.upenn.edu.

10.1021/jp051068+ CCC: $30.25
Published on Web 09/08/2005

tions are described in a review from our group.[21] In addition to being useful for investigations of biomolecule−water interactions, temperature-dependent infrared spectroscopy can also be used to examine the bulk solvent pool itself. By measurement of the changes in peak position and area, temperature-dependent IR allows direct measurement of hydrogen bonding using correlations that have already been determined[23] and through the application of a simple new analysis presented here. The power of this method for investigating H-bonding systems makes it ideally suited to investigate the H-bonding properties of reverse micellar water pools of varying sizes.

Materials and Methods

Reverse micelles were prepared by dissolving bis(2-ethylhexyl) sulfosuccinate (AOT), Sigma grade (Sigma-Aldrich, St. Louis, MO), in *n*-pentane (Sigma-Aldrich), at 75 mM (for $w_o = 40$) or 150 mM (for $w_o = 1$, 2, 5, 8, 10, 20, and 30), and adding the appropriate volume of H_2O or D_2O (Cambridge Isotope Laboratories, Inc., Andover, MA) for w_o of 1, 2, 5, 8, 10, 20, 30, or 40. All RM samples were single phase and optically clear. Samples were sealed between two CaF_2 windows of 2.54 cm diameter by 1 or 2 mm thickness with no spacer. The thickness of the sample was determined interferometrically to be 9 μm. Samples at $w_o = 1$, 2, and 8 were prepared only with D_2O water pools and were only measured at room temperature for determination of the appropriate frequencies for fitting the spectral components. All other w_o values were prepared with both H_2O and D_2O water pools and were used for the full TEIR (temperature excursion IR) analysis. The infrared spectra were recorded on a Bruker IFS 66 Fourier transform infrared spectrometer (Bruker, Brookline, MA) at 5 K intervals from room temperature to 220 K with temperature modulated by an ADP closed cycle Helitran cryostat (Advanced Research Systems, Allentown, PA) and a Scientific Instruments model 9650 temperature controller (Scientific Instruments, West Palm Beach, FL). Bulk water was also analyzed using this equipment and temperature range. D_2O with 1% H_2O (v/v) was used for the bulk O−H analysis, and H_2O with 2% D_2O was used for the bulk O−D analysis. Though it would be preferable to use pure H_2O and D_2O for these measurements in order to compare the RM spectra with that of vibrationally coupled water, the absorption signals of the O−H and O−D stretching vibrations are so strong as to prohibit such measurements from being on-scale, despite the thinness of the sample.

Spectra were analyzed with Opus 5.0 (Bruker) and spectral decomposition was performed with PeakFit 4.11 (SYSTAT Software, Inc., Richmond, CA). For D_2O samples, the contributions of AOT and pentane were subtracted from the O−D stretching region before fitting analysis. The O−H or O−D stretching regions were fit to a series of three Gaussians. The spectral fits were performed using PeakFit, starting with a Gaussian at each of the three accepted[14] frequencies for the O−H stretching components, 3603 ± 6, 3465 ± 5, and 3330 ± 20 cm^{-1}, or their O−D equivalents, 2650 ± 5, 2565 ± 15, and 2460 ± 20 cm^{-1}, determined through analysis of the O−D stretching vibration with increasing w_o (see Results for description). The areas of these components were then used to analyze the H-bond network behavior of the RM water pool with changing temperature.

A two-state model was used to quantitatively compare the spectra of the varied w_o RM water pools. This model is based on analyses performed by Sharp and colleagues, which demonstrated that water treated as a random network still exhibits two main H-bond angular populations centered at 12° (low angle, nearly linear) and 54° (high angle, strained).[24−30] By using the areas of the low frequency (low angle) and intermediate frequency (high angle) components as the relative populations of H-bonds in each configuration, the effective equilibrium constant of conversion from high angle to low angle was calculated by: $K_{h\rightarrow l} = A_l/A_h$, where A_l is the area of the low-frequency component and A_h is the area of the intermediate frequency component. This constant was then used to calculate an effective energy difference between the H-bond conformations with the Boltzmann relationship for free energy: $\Delta G = -kT \ln K$, where k is Boltzmann's constant and T is the temperature in degrees kelvin. These energies were then compared between the samples with respect to temperature to observe the differences in behavior of the RM water pool H-bond network as a function of w_o.

Results

Reverse Micellar Water in the Liquid Phase. AOT reverse micelles were prepared with H_2O and with D_2O at $w_o = 5$, 10, 20, 30, and 40. The infrared spectra of these samples were recorded from 295 to 220 K at 5 K intervals. These spectra were compared to the spectrum of bulk O−H to compare the behavior of encapsulated water to that of free aqueous solution (Figure 1, H_2O; Figure 2, D_2O). The temperature dependence of the reverse micelle spectra grew increasingly similar to the spectra of bulk water as w_o increased; with increasing w_o, the shift to lower frequency of the O−H stretch was more dramatic and better defined. At maximum w_o, peak shape and frequency shift were the same as those of bulk water. At $w_o = 10$ (the lowest w_o with an appreciable bulklike water population[2]), the temperature dependence was markedly different than that in the higher w_o samples. At $w_o = 5$, no temperature-dependent changes in the O−H stretching vibration were observed.

The O−H and O−D stretching regions of the RM spectra were fit to three (high, intermediate, and low frequency) Gaussian components, corresponding to surfactant-bound water, high-angle H-bonds in the bulklike water, and low-angle H-bonds in the bulklike water, respectively. This fitting procedure was straightforward for the H_2O samples, utilizing the previously assigned component frequencies discussed above (Figure 3). Fitting the O−D stretch for the D_2O samples was much less straightforward. Conversion of the frequencies of the O−H stretch components using the reduced mass ratio failed to provide reproducible fits. Instead, the approach used previously[14] to assign the components of the O−H stretch was used to assign component frequencies for the O−D stretch.

Reverse micelles with D_2O at $w_o = 1$, 2, 5, 8, 10, 20, 30, and 40 were prepared and their spectra at room temperature were compared (Figure 4A). These spectra were each fit to three components, yielding the following frequency range assignments: 2650 ± 5 cm^{-1} for surfactant bound water, 2565 ± 15 cm^{-1} for bulklike water high-angle H-bonds, and 2460 ± 20 cm^{-1} for bulklike water low-angle H-bonds (Figure 4B). All spectra above the phase transition temperature were fit with these components. The frequencies of the final fits are shown in Table 1.

Energetics of the Reverse Micelle Water Hydrogen Bonding Network. The areas of the Gaussian components were used to perform an energetic analysis of the hydrogen bond network behavior of the bulklike RM water population. This analysis employed a simple treatment of the bulklike water pool as a two-state system of low-angle H-bonds and high-angle H-bonds as used previously by Sharp and colleagues for computational analyses[24−31] (see Discussion for a more extensive description).

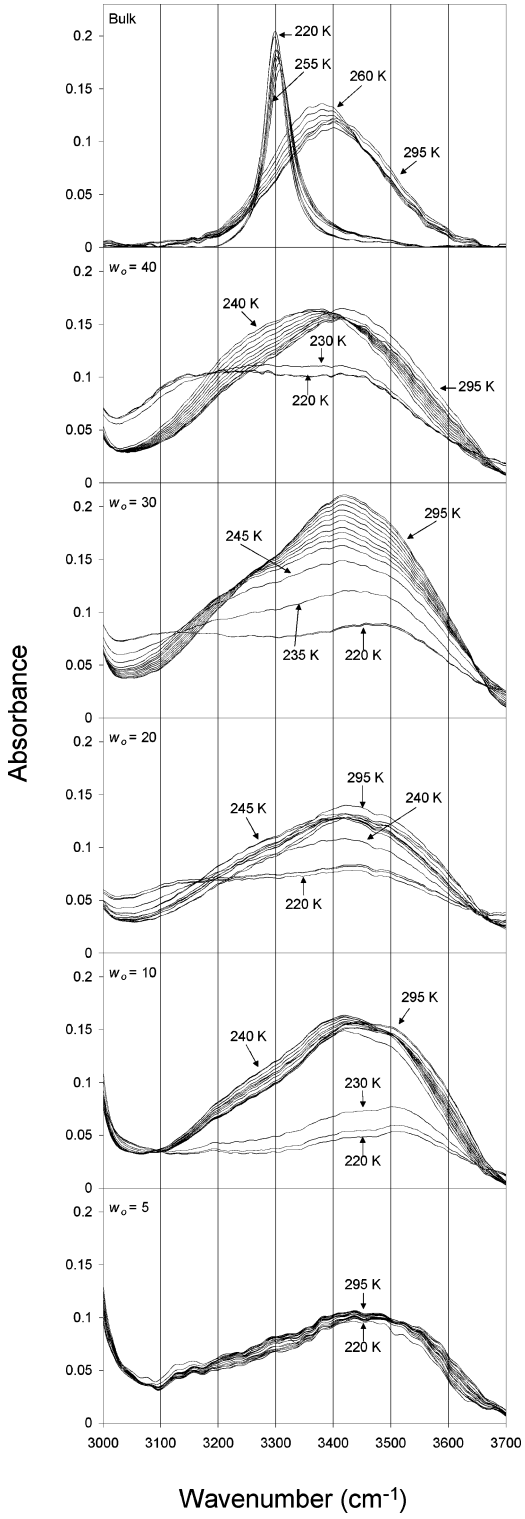

Figure 1. Temperature-dependent infrared spectra of reverse micelles with H_2O at varied w_o. The spectra of bulk water above 255 K and the spectra of $w_o = 5$ were multiplied by 3 and 4, respectively.

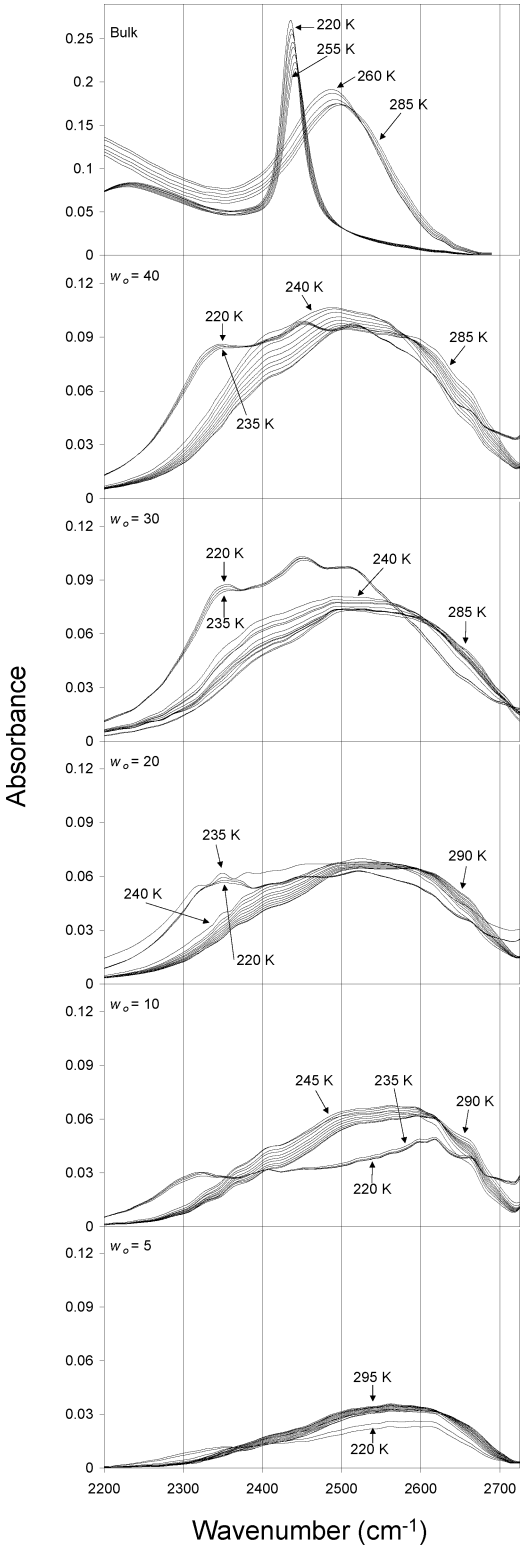

Figure 2. Temperature-dependent infrared spectra of reverse micelles with D_2O at varied w_o. The spectra of bulk water above 255 K were multiplied by 4.

Briefly, the areas of the low and intermediate frequency components were considered to represent the relative populations of low-angle and high-angle H-bonds, respectively, in the sample. Equilibrium constants for the conversion from high-angle to low-angle H-bond were calculated from these relative populations. Effective free energy differences between the two H-bond angles at each temperature point under each condition were then determined from the equilibrium constants. Though these energy values do not provide absolute quantitation of the water pool energies, they clearly demonstrate the comparative behavior of the RM water pools with varying size and temperature.

The results of the energetic analysis are shown in Figure 5 for all temperatures at which the sample remained fully liquid. At $w_o = 5$, high angle H-bonding was energetically favored at all temperatures for both H_2O and D_2O. At $w_o \geq 10$, low-angle H-bonds were energetically favored. These data are consistent

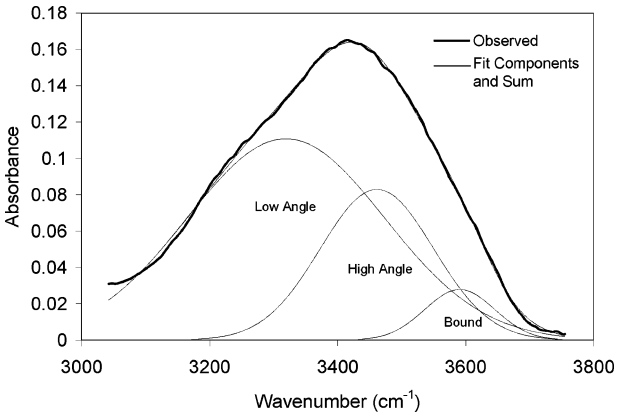

Figure 3. Gaussian components of the O−H stretching vibration of H_2O in reverse micelles at $w_o = 40$. The components are located at: surfactant bound, 3603 ± 6 cm^{-1}; high angle, 3465 ± 5 cm^{-1}; low angle, 3330 ± 20 cm^{-1}.

with previous examinations of RM water showing that bulklike water in the RM core appears at $w_o \geq 6$; thus, at $w_o = 5$, all water is effected by, though not necessarily bound to, the surfactant layer. As w_o increased, the free energy difference between the H-bond configurations approached that seen in bulk water. This was true across the full temperature range in which bulk water could be measured before freezing. The H-bond network behavior of bulk water was only replicated by the highest $w_o = 40$. These data clearly demonstrate that the H-bond network of RM water at $w_o = 20$ behaves quite differently than that of bulk water.

Reverse Micellar Water below Phase Transition Temperature. All RM samples with $w_o \geq 10$ exhibited a shift in the spectra between 235 and 245 K corresponding to a phase change. At $w_o = 20$, 30, and 40, the phase transition showed an overall shift toward lower frequency, as seen in the freezing of bulk water, but the spectra did not sharpen as does the absorption of bulk ice. At $w_o = 10$ with H_2O there was no shift to lower frequency, but rather an overall drop in intensity, the same effect as was seen for $w_o = 5$ with D_2O. The spectrum of $w_o = 5$ with H_2O showed no temperature-dependent changes at or below the phase transition temperature, suggesting that this sample did not under go a phase change between 235 and 245 K.

To obtain a more accurate understanding of what happens to the RM system at the phase transition temperature, the w_o-sensitive complex absorption of AOT centered at 1240 cm^{-1} was used to monitor water content of the RM samples (Figure 6). This mode is composed of the overlapping CH_2 twist, SO_3 antisymmetric stretch, and ester C−O stretch.[8] As shown in Figure 6A, this mode changes markedly with increasing w_o from 0 to 8, though it does not change drastically above $w_o = 8$ (not shown). As is readily evident, this absorption at $w_o = 0$ was dominated by two modes at 1214 and ∼1250 cm^{-1}. These shifted closer to one another with increasing w_o. A comparison of these room-temperature spectra at low w_o with the room-temperature and low-temperature spectra of RM at higher w_o reveals that even below the phase transition temperature, surfactant remains water associated in all RM samples tested.

Shown in Figure 6B are the high- and low-temperature spectra for reverse micelles at $w_o = 5$ and 20 as well as the room-temperature spectra of RM with $w_o = 2$ and 0. In all of the spectra, the surfactant mode was somewhat obscured by a pentane mode at 1258 cm^{-1}, seen most prominently as the highest frequency peak in the spectrum for $w_o = 5$ at 220 K. This mode does not shift but increases in amplitude with decreasing temperature (not shown). The high- and low-temperature spectra at $w_o = 5$ show no differences in peak position but only sharpening of the spectrum and an increase in amplitude of the pentane mode at low temperature. This lack of change in the water-sensitive surfactant mode and the lack of phase change shift in the O−H stretching mode demonstrate that reverse micelles at $w_o = 5$ do not undergo a low-temperature phase transition and that at low temperature the water pool remains encapsulated by surfactant. The high- and low-temperature spectra at $w_o = 20$, however, show a marked shift from high to low temperature. This shift occurs entirely between 245 and 235 K (not shown). Comparison of the low-temperature $w_o = 20$ spectrum with the spectra of RM with $w_o = 0$ and 2 shows that the surfactant peak positions of the low temperature $w_o = 20$ reverse micelle sample, ∼1219 and 1243 cm^{-1}, closely resemble the spectrum of $w_o = 2$, 1219 and 1243 cm^{-1}, and do not resemble the spectrum of $w_o = 0$. This is strong evidence that, though the majority of the water comes out of the reverse micelle and freezes at the phase transition temperature, a small amount of water remains encapsulated. This similarity to $w_o = 2$ was seen for the low-temperature spectra of all samples at $w_o > 5$.

Discussion

Reverse micelles are a widely used system for many different types of investigations, from facilitating organic syntheses to structural analysis of biomolecules. Reverse micelles are useful because they allow sequestering of the molecule or molecules of interest in a small water pool. Because of their utility, the properties of reverse micelles have been extensively investigated, often with particular focus on the reverse micellar water pool. Reverse micelles have also been used as a tool to describe the nanoscale behavior of water networks.[8] Though the H-bonding population character of the RM water pool has been described at room temperature, the temperature dependence of this property has not previously been described.

We have examined the O−H and O−D stretching vibrations of RM water pools with pure H_2O and pure D_2O from room temperature to 220 K. The respective stretching vibrations were analyzed using deconvolution into three Gaussian populations representing three types of H-bonded water following the procedure of Onori and Santucci.[14] By analyzing the O−H/D stretch over a range of temperatures with this deconvolution, we observed the population shift of RM water between H-bonding conformations with temperature. These data offer a highly sensitive and detailed means of examining water structure in the confined environment of a reverse micelle. Our data demonstrate that the behavior of RM water is markedly different from bulk aqueous solution at $w_o < 40$ and that the freezing of the RM water pool is not dependent on w_o.

Spectral Resolution. There are a variety of factors affecting spectral resolution that must be considered in analyzing the present data. The vibrational lifetime of the O−H stretching mode, τ_{OH}, of water is temperature dependent, with τ_{OH} decreasing with decreasing temperature, from ∼0.9 ps at 350 K to ∼0.8 ps at 270 K, and τ_{OH} of ice is less than half the value for liquid water, ∼0.38 ps, but virtually independent of temperature.[32] Because of this unique vibrational behavior, the O−H stretch absorption of liquid water becomes increasingly uncertainty broadened as temperature drops, while that of ice is far more uncertainty broadened compared to water but does not become more broadened with dropping temperature. There is also a dependence of τ_{OH} on w_o, with τ_{OH} decreasing as w_o is reduced.[18] Though the precise extent of this dependence has

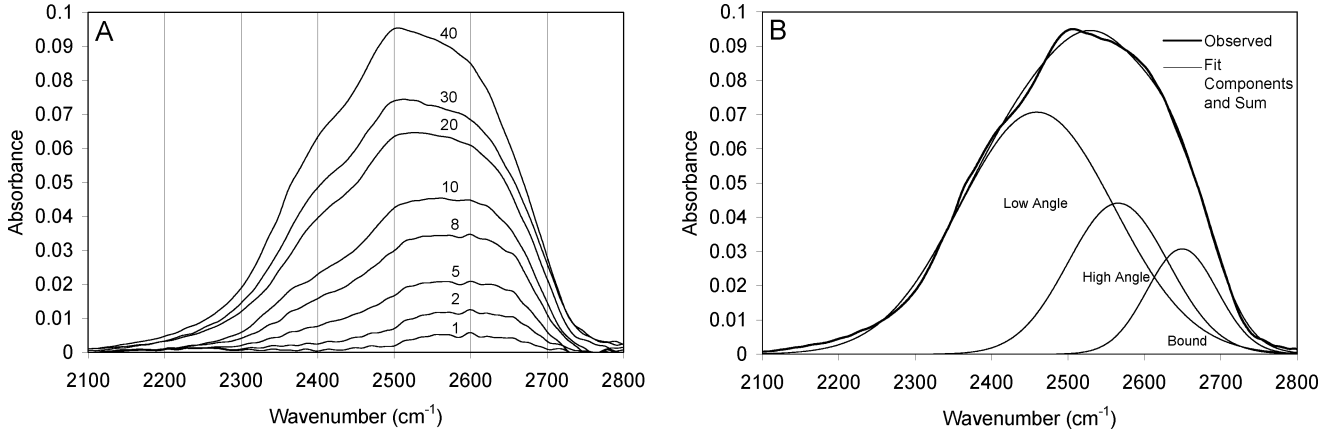

Figure 4. (A) The O−D stretching vibration of reverse micellar D_2O at varied w_o. (B) The O−D stretch vibrational components as determined by fitting the spectra in (A). O−D components are at: surfactant bound, 2650 ± 5 cm^{-1}; high angle, 2565 ± 15 cm^{-1}; low angle, 2460 ± 20 cm^{-1}.

TABLE 1: Frequency Ranges (cm^{-1}) of Gaussian Components Fit to the O−H and O−D Stretching Modes of Reverse Micellar Water Pools at Varied w_o

	H_2O			D_2O		
w_o	low angle	high angle	bound	low angle	high angle	bound
5	3323 ± 8	3489 ± 2	3594 ± 1	2449 ± 1	2568 ± 9	2650 ± 1
10	3305 ± 3	3481 ± 4	3598 ± 4	2468 ± 6	2572 ± 14	2648 ± 3
20	3305 ± 12	3476 ± 4	3595 ± 2	2434 ± 18	2565 ± 6	2649 ± 1
30	3310 ± 11	3467 ± 1	3594 ± 1	2450 ± 6	2558 ± 1	2649 ± 1
40	3321 ± 3	3464 ± 3	3595 ± 5	2459 ± 1	2570 ± 5	2469 ± 1
Bulk	3367 ± 10	3453 ± 3	3596 ± 3	2480 ± 5	2535 ± 1	

not been determined, it has been shown to be less than a tenth of a picosecond.[18] The minimum line width of the OH stretch at 350 K is ∼2.3 cm^{-1}, while at 270 K it is ∼2.6 cm^{-1}. In ice, the minimum line width is ∼5.2 cm^{-1}. The dependence of τ_{OH} on w_o causes a maximum line width dependence in the liquid phase of ∼1 cm^{-1}. The vibrational modes evaluated here have widths of 200−400 cm^{-1} and the fit functions have widths of at least 50 cm^{-1}, so the broadening as a result of the temperature dependence of τ_{OH} is insignificant since the line widths under all conditions are far less than the width of the modes of interest. The effect of w_o on τ_{OH} causes a maximum change in line width of ∼0.4 cm^{-1}, thus this effect is negligible when considering these data.

Treatment of Water as a Two-State System. Many models have been proposed for description of water behavior over the past 50 years. Most prominently, there has been considerable debate over whether water may be analyzed as a two-state mixture of icelike water clusters and non-H-bonded water molecules or as a continuous network of H-bonds of randomly distributed lengths and angles.[33] In the past few years, Sharp and colleagues have analyzed computational simulations of water, treating liquid water as a random H-bond network.[24−29,31] They have demonstrated that the random network model of water yields an O−O radial distribution function which closely replicates that seen in experiments. This distribution function suggests that there is a first-shell coordination level of H-bonding in liquid water, but defined populations of water "types" do not exist beyond that first neighbor. Analysis of the H-bond angular distribution function in these same simulations, however, clearly demonstrates the existence of two high-probability regions of the continuum H-bond angular distribution function centered at 12°, a nearly linear icelike H-bond, and at 54°, a high-angle more strained H-bond.

The findings of Sharp et al. suggest that the O−H stretching vibration of liquid water can be analyzed effectively as a two-state system of low-angle and high-angle H-bonds. The low-angle H-bond population corresponds to the low-frequency icelike component used in previous IR fitting procedures at ∼3330 cm^{-1}. The high-angle H-bond population corresponds to the higher frequency component used previously at ∼3465 cm^{-1}. This two-state treatment is admittedly a vast simplification of the O−H stretching vibrational spectra, and it should be clarified that our treatment of the spectra in this manner is not an application of a mixture model of water. This analysis does not classify the water into icelike and free categories but rather classifies the hydrogen bonds as low angle and high angle. Though this may seem a subtle difference, it is essential to understand that this analysis still considers water as a continuous network. This model simplifies a complex problem and proves an effective method for quantitatively describing spectral differences in terms of free energy differences between H-bond conformational states in the samples. The energy values obtained with this analysis are not absolute energies but rather energy differences between these states of water under different conditions. This type of comparison provides a clear and powerful means of determining the effects of environment on water.

Liquid Reverse Micellar Water. Analysis of the temperature dependence of RM water at various water loadings between room temperature and 245 K demonstrates that RM water is less susceptible to temperature-related perturbation than bulk water, that its sensitivity to such perturbation increases with w_o, and that the H-bonding population behavior in response to temperature change does not approximate bulk water until the highest w_o. At room temperature, our infrared RM water spectra replicate previous results well with the bulk water population increasing in area with increasing w_o while the amount of bound water remains essentially stable.[14,16] At $w_o \geq 20$, the O−H stretch absorption closely mimics that of bulk water at room temperature. A more rigorous analysis of the spectra, using the three Gaussian component decomposition established previously,[11,14] shows that, despite the similarity of the RM water

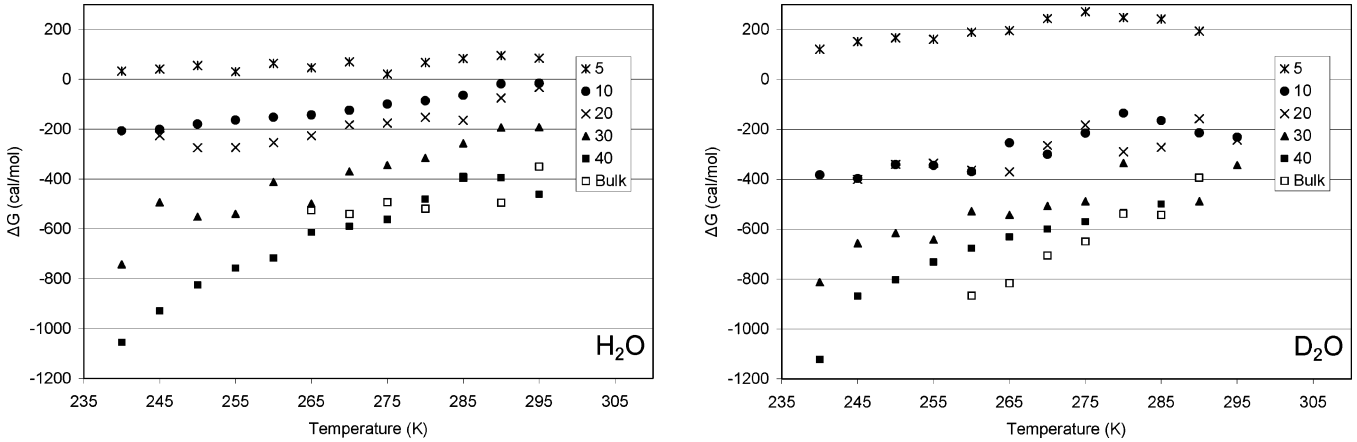

Figure 5. Free energy analysis of the transition from high-angle H-bonding to low-angle H-bonding for (A) reverse micelles with H_2O at varied w_o and for (B) reverse micelles with D_2O at varied w_o.

spectra to bulk spectra at room temperature, the temperature-dependent behavior is drastically different and highly dependent on w_o.

In bulk water and in all RM samples with $w_o \geq 20$ at all temperatures above 235 K, a vast majority of the total water is in the high- and low-angle populations for both H_2O and D_2O water pools. At $w_o = 10$, the H-bond population distribution is much more even, with a much larger percentage of the total water in the high-frequency, bound water, population. At $w_o = 5$, there are no temperature-dependent spectral changes save a minor drop in amplitude at the phase transition temperature for the D_2O water pool. At this low w_o, the low-angle population is decidedly lower than the high-angle population at all temperatures. This is consistent with previous analyses of RM hydration that have shown that the core bulk water pool does not grow until $w_o \geq \sim 6$ because the surfactant headgroups are not fully hydrated until above this w_o.[16] With decreasing temperature, the water populations are driven to stronger H-bonding conformations, i.e., more linear H-bonds, increasing population of the low-angle H-bond component. This trend is seen in all samples, but it is barely evident at $w_o = 5$ and becomes increasingly dramatic with increasing w_o. This is most obviously seen through the free energy analysis (Figure 5) where the energy difference between conformations drops by less than 100 cal/mol over the full temperature range for $w_o = 5$. This drop in ΔG is increasingly dramatic as w_o increases, with the maximum change with temperature being ~650 cal/mol for $w_o = 40$. The energetic analysis also shows that the behavior of the H-bond network of water and the D-bond network of D_2O closely mimic each other. The trends of temperature dependence of ΔG are the same, and the energy differences are in all cases quite similar. The free energy differences between high- and low-angle bonds for D_2O do appear to be systematically lower than for H_2O at all $w_o \geq 10$. This is not unexpected since the linear D-bond is stronger than the linear H-bond due to the difference in zero point energy.[34] This increased strength likely makes the linear D-bond slightly more favorable in most conditions than the linear H-bond.

The temperature-dependent H-bonding population behavior of RM water gives strong evidence that water in confined space below a certain size is less susceptible to temperature-related rearrangement than bulk water. The larger the water pool becomes, the more easily the water rearranges to assume lower energy H-bonding conformations at lower temperature. Recently, reverse micelles have been used to examine the effect of nanoscale confinement on the water H-bond network, but these investigations have investigated reverse micelles at $w_o \leq 12$, corresponding to a water pool with a maximum diameter of about 4 nm.[3−5] Our data suggest that spatial restriction effects the water H-bond network on a much larger scale than is accessible at $w_o = 12$, perhaps on a scale almost four times as large. This insight into the size-dependence of the water H-bond network is of interest, but of equal interest is the potential for the methodologies used here for future investigations of water structure and solvation.

IR is an excellent tool for measuring H-bonding of water populations and has recently been combined with reverse micelles to examine water structure around nanoparticles.[15] Temperature-dependent IR offers an extra dimension of water structure examination, allowing an in-depth analysis of water structure around reverse-micelle-solubilized molecules. The two-state model free energy analysis of the water H-bond network that we have used here allows the very difficult problem of water structure to be simplified yet still dealt with in a highly quantitative way. In addition to demonstrating the dependence of RM water H-bonding population behavior on w_o, the present data provide an important foundation for the combination of temperature-dependent IR, reverse micelles, and decomposition free energy analysis to examine water structure around biological molecules, an investigation currently underway in our laboratory.

Reverse Micellar Water below the Phase Transition Temperature. The thinness of the sample in our setup causes bulk water to be supercooled such that it does not freeze until between 260 and 255 K. All of the reverse micelle samples showed phase transition near 240 K. This reverse-micelle-induced supercooling has been observed previously, and our freezing point value for the RM water pool, ~ −35 °C, is in close agreement with previously reported values.[35] This supercooling behavior of RM water is not unexpected given the results discussed above for liquid RM water. The resistance of the RM water pool to temperature-related perturbation as compared to bulk water would predict that the freezing of RM water would take place at a lower temperature than that of bulk water.

The freezing point and freezing behavior of RM water are subjects of interest for cryoenzymology and low-temperature structural biology.[36,37] The freezing of RM water has received specific attention recently in an extensive investigation using fluorescent probes to monitor the temperature dependence of various parts of the RM environment.[38] This report describes a w_o-dependent freezing of the RM water pool that our results contradict. Munson et al. suggest that the freezing point of the core of the water pool is dependent on w_o, ranges from −10 to −60 °C, and decreases with decreasing w_o.[38] Our spectra show

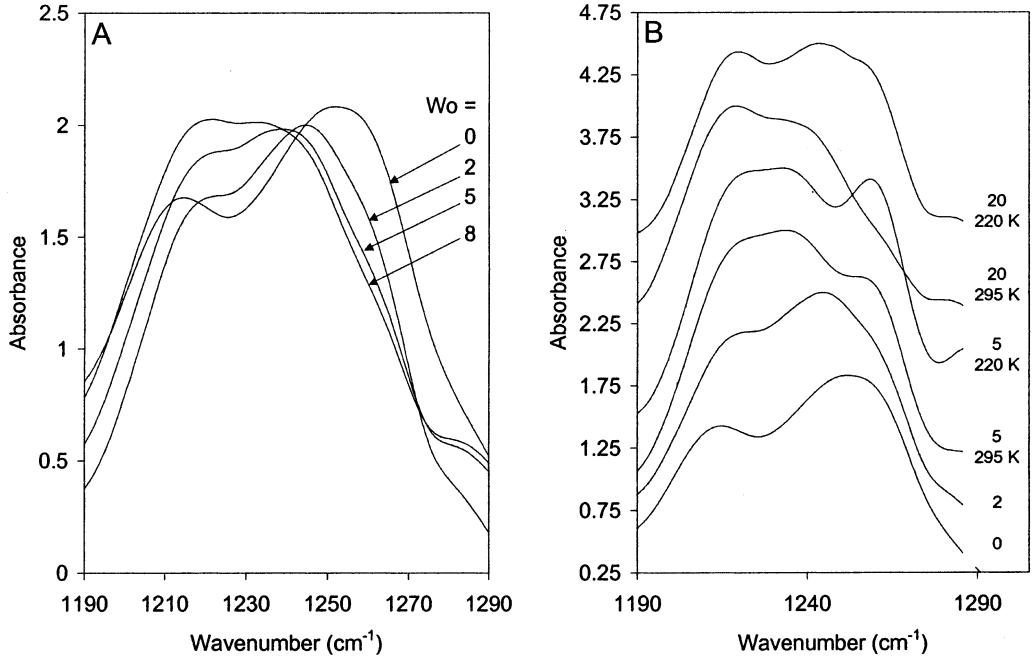

Figure 6. (A) AOT combination mode at various w_o at room temperature. (B) Stacked spectra of the AOT combination mode under various w_o and temperatures. Spectra at $w_o = 0$ and 2 are at room temperature.

that there is clearly a phase transition of the RM water in a similar temperature range, but this phase transition occurs within a 10 K range, 245 to 235 K, regardless of w_o. There is no evidence in our spectra that the freezing temperature of any portion of the water pool is w_o -dependent, as the spectra remain essentially constant to 200 K (not shown).

The phase transition of the RM water in our experiments is quite evidently different than the freezing of bulk water. Vibrationally decoupled bulk ice yields an O−H/D stretching vibration that is sharp and homogeneous, as shown in Figures 1 and 2 and as described by Zelent et al.[39] The spectra of frozen RM water are clearly quite different from bulk ice under all conditions tested. These spectra show a shift to lower frequency upon freezing, as seen in bulk ice, but unlike bulk ice, the O−H/D stretch is quite broad and clearly composed of multiple components, indicating that the RM water does not freeze into a continuous ice crystal. The freezing of RM water shows a clear dependence on w_o with respect to its spectral similarity to bulk ice. For both types of water pool, with increasing w_o, the population of water molecules in the icelike component grows. Even at the highest w_o, though, this icelike component has a slightly different frequency and a drastically different width than that seen in bulk ice. The only exception to this trend is the $w_o = 10$, H_2O sample. The phase transition for this sample exhibits no shift to lower frequency but instead merely drops in intensity. The proposed explanation for this is addressed below.

Elucidation of the process by which RM water freezes may help improve understanding of RM behavior at low temperature, facilitating design of better RM systems for low-temperature experiments. On the basis of several points in the literature and our spectra of AOT RM samples at low temperature, we propose that the bulklike RM water spontaneously falls out of the reverse micelles at around −35 °C, forming smaller reverse micelles that have a very low hydration level and leaving the majority of the RM water pool in a small cluster suspended in nonpolar solvent. This small water cluster rapidly freezes in the low-temperature organic solvent and precipitates. This suggested process is based not only on the behavior of the O−H stretching mode, which is temperature independent at low w_o and strongly resembles the spectra of ice nanocrystals,[40,41] but also on the w_o-sensitive AOT mode in Figure 6, which clearly demonstrates that the AOT in subfreezing RM samples remains water associated.

Many studies on AOT reverse micelles at low temperature have noted the low freezing point of the RM water pool.[35] It has also been well established that water loading in AOT reverse micelles is an entropically driven process;[35,42−44] thus it is reasonable to expect that there would be a low temperature at which the entropically favorable encapsulation of water in the reverse micelle would no longer be enough of a contribution to the free energy of the mixture to keep the reverse micelles in tact. At low temperature, the RM sample is governed by enthalpically favored interactions, which have been identified and discussed at length by Shen et al. as solvation of the surfactant headgroups and counterions in AOT reverse micelles. Combined with these previous findings, the present data suggest that the low-temperature destabilization of AOT RM structure results in the release and phase-separation of bulklike water while the bound water layer is maintained, resulting in free water and smaller reverse micelles with lower w_o. This model would dictate that the small water pools released from the RM core at low temperature would rapidly freeze once free from encapsulation.

On the basis of a rough estimation using the average surface area of a fully hydrated AOT headgroup (55 Å^2) and the average volume of a water molecule (30 Å^3), the radius of the bulk water pool in our RM samples ranged from ∼1 nm ($w_o = 10$) to ∼7 nm ($w_o = 40$). The infrared spectra of frozen water clusters in this size range have been characterized, and these spectra look remarkably similar to our spectra of frozen RM water.[40,41] The O−D stretching region of large D_2O clusters formed with low-temperature vapor deposition have a very similar three-component profile to the spectra of frozen RM D_2O, and the magnitude of those components varies with cluster size in a fashion very similar to the variation of the frozen RM water spectra with w_o.[40,41] Not only does the overall behavior of the frozen water cluster spectra closely mimic that of frozen RM water, but the component frequencies correspond remarkably well with those seen in the O−D stretching regions of frozen RM D_2O. The frozen water clusters were shown to be composed

of a central crystal core surrounded by a disordered surface layer.[40] The smallest cluster size tested, 2 nm, was found to be quite near the lower limit for formation of a central crystal.[40] This is approximately the size estimate for the RM water pool at $w_o = 10$, thus the absence of a shift to lower frequency of the O−H stretching vibration in this sample could be explained by the free RM water pool being too small for formation of a central crystal. Rather, this water pool may freeze into an amorphous solid water cluster, the O−H stretching spectrum of which would be composed of higher frequency modes due to its distorted H-bonds.

These data demonstrate that the low-temperature phase transition of reverse micelles is not dependent on w_o. The proposed model for low-temperature behavior of AOT RM systems suggests that better low-temperature RM systems may be possible using alternative surfactants or surfactant mixtures. Considering that the favorable entropy of water loading in AOT is insufficient to maintain the RM structure fully at low temperature, alternative surfactants or surfactant mixtures in which the endothermic contributions to the water loading energies are lessened, such as the network interaction between the headgroup and counterion, should maintain the RM structure better at low temperatures.

Summary

The temperature-dependent infrared absorption of reverse micellar water pools was measured from room temperature to 220 K at a variety of w_o under varied D/H isotopic ratios. In the liquid phase, the RM water pool H-bond network energetically favored low-angle H-bonds less than in bulk water, and this behavior was w_o-dependent, approaching that of bulk water with increasing w_o. The freezing of RM water pools was observed and found to be independent of w_o, occurring at ~ -35 °C in all samples. The spectra of subfreezing RM samples were informative and allowed the proposal of a model for low-temperature behavior of AOT reverse micelles that accounts for the peculiarities of this behavior and could aid in design of better low-temperature RM systems. The methodologies and model for water treatment used here lay the groundwork for the use of reverse micelles and temperature-dependent IR in the future study of liquid water structure around solvated molecules, an avenue of investigation currently being pursued by our group.

Acknowledgment. We thank Drs. A. Joshua Wand, Kim Sharp, Kathleen Valentine, Mazdak Khajehpour, Bogumil Zelent, Ronald Peterson, and Jennifer Dashnau for helpful discussions. Funding support was provided by the National Institutes of Health, Grant PO1 GM 48130.

References and Notes

(1) Chang, G.-G.; Huang, T.-M.; Hung, H.-C. Reverse Micelles as Life-Mimicking Systems. *Proc. Natl. Sci. Counc., Repub. China, Part A: Phys. Sci. Eng.* **2000**, *24* (3), 89−100.

(2) De, K. T.; Maitra, A. Solution behaviour of Aerosol OT in nonpolar solvents. *Adv. Colloid. Interface Sci.* **1995**, *59*, 95−193.

(3) Dokter, A. M.; Woutersen, S.; Bakker, H. J. Anomalous Slowing Down of the Vibrational Relaxation of Liquid Water upon Nanoscale Confinement. *Phys. Rev. Lett.* **2005**, *94* (17).

(4) Tan, H.-S.; Piletic, I. R.; Riter, R. E.; Levinger, N. E.; Fayer, M. D. Dynamics of Water Confined on a Nanometer Length Scale in Reverse Micelles: Ultrafast Infrared Vibrational Echo Spectroscopy. *Phys. Rev. Lett.* **2005**, *94* (5).

(5) Harpham, M. R.; Ladanyi, B. M.; Levinger, N. E.; Herwig, K. W. Water motion in reverse micelles studied by quasielastic neutron scattering and molecular dynamics simulations. *J. Chem. Phys.* **2004**, *121* (16), 7855−7868.

(6) D'Aprano, A.; Lizzio, A.; Liveri, V. T.; Aliotta, F.; Vasi, C.; Migliardo, P. Aggregation States of Water in Reversed AOT Micelles: Raman Evidence. *J. Phys. Chem.* **1988**, *92*, 4436−4439.

(7) Temsamani, M. B.; Maeck, M.; Hassani, I. E.; Hurwitz, H. D. Fourier Transform Infrared Investigation of Water States in Aerosol-OT Reverse Micelles as a Function of Counterionic Nature. *J. Phys. Chem. B* **1998**, *102*, 3335−3340.

(8) Jain, T. K.; Varshney, M.; Maitra, A. Structural Studies of Aerosol OT Reverse Micellar Aggregates by FT-IR Spectroscopy. *J. Phys. Chem.* **1989**, *93*, 7409−7416.

(9) Haandrikman, G.; Daane, G. J. R.; Kerkhof, F. J. M.; van Os, N. M.; Rupert, L. A. M. Microcalorimetric Investigation of the Solubilization of Water in Reversed Micelles and Water-in-Oil Microemulsions. *J. Phys. Chem.* **1992**, *96*, 9061−9068.

(10) Di Profio, P.; Germani, R.; Onori, G.; Santucci, A.; Savelli, G.; Bunton, C. A. Relation between the Infrared Spectrum of Water and Decarboxylation Kinetics in Cetyltrimethylammonium Bromide in Dichloromethane. *Langmuir* **1998**, *14*, 768−772.

(11) Brubach, J.-B.; Mermet, A.; Filabozzi, A.; et al. Dependence of Water Dynamics on Confinement Size. *J. Phys. Chem. B* **2001**, *105*, 430−435.

(12) Zhou, N.; Li, Q.; Wu, J.; Chen, J.; Weng, S.; Xu, G. Spectroscopic Characterization of Solubilized Water in Reversed Micelles and Microemulsions: Sodium Bis(2-ethylhexyl) Sulfosuccinate and sodium Bis(2-ehtylhexyl) Phosphate in *n*-Heptane. *Langmuir* **2001**, *17*, 4505−4509.

(13) Li, Q.; Weng, S.; Wu, J.; Zhou, N. Comparative Study on Structure of Solubilized Water in Reversed Micelles. 1. FT-IR Spectroscopic Evidence of Water/AOT/*n*-Heptane and Water/NaDEHP/*n*-Heptane Systems. *J. Chem. Phys. B* **1998**, *102*, 3168−3174.

(14) Onori, G.; Santucci, A. IR Investigations of Water Structure in Aerosol OT Reverse Micellar Aggregates. *J. Phys. Chem.* **1993**, *97*, 5430−5434.

(15) Nickolov, Z. S.; Paruchuri, V.; Shah, D. O.; Miller, J. D. FTIR-ATR studies of water structure in reverst micelles during the synthesis of oxalate precursor nanoparticles. *Colloids Surf., A* **2004**, *232*, 93−99.

(16) Freda, M.; Onori, G.; Paciaroni, A.; Santucci A. Hydration and dynamics of Aerosol OT reverse micelles. *J. Mol. Liquids* **2002**, *101*, 55−68.

(17) Patzlaff, T.; Janich, M.; Seifert, G.; Graener, H. Ultrafast dynamics of water-AOT-octane microemulsions. *Chem. Phys.* **2000**, *261*, 381−389.

(18) Seifert, G.; Patzlaff, T.; Graener, H. Size Dependent Ultrafast Cooling of Water Droplets in Microemulsions by Picosecond Infrared Spectroscopy. *Phys. Rev. Lett.* **2002**, *88* (14).

(19) Robinson, E. A.; Schreiber, H. D.; Spencer, J. N. Solvent and Temperature Effects on the Hydrogen Bond. *J. Phys. Chem.* **1971**, *76* (14), 2219−2222.

(20) Schroeder. L. R.; Cooper, S. L. Hydrogen bonding in polyamides. *J. Appl. Phys.* **1976**, *47* (10), 4310−4316.

(21) Vanderkooi, J. M.; Dashnau, J. L.; Zelent, B. Temperature excursion infrared spectroscopy used to study hydrogen bonding between water and biomolecules. *Biochim. Biophys. Acta* **2005**, *1749*, 214−233.

(22) Nucci, N. V.; Zelent, B.; Vanderkooi, J. M. Temperature Gradient Infrared Spectroscopy as a Method for Investigation of Protein-Water Interaction. *Biophys. J.* 2004; Annual Meeting Abstracts: 1668-Pos.

(23) Novak, A. Hydrogen Bonding in Solids. Correlation of Spectroscopic and Crystallographic Data. *Struct. Bonding* **1974**, *18*, 177−216.

(24) Madan, B.; Sharp, K. Heat Capacity Changes Accompanying Hydrophobic and Ionic Solvation: A Monte Carlo and Random Network Model Study. *J. Phys. Chem.* **1996**, *100*, 7713−7721.

(25) Madan, B.; Sharp, K. Molecular Origin of Hydration Heat Capacity Changes of Hydrophobic Solutes: Perturbation of Water Structure around Alkanes. *J. Phys. Chem. B* **1997**, *101*, 11237−11242.

(26) Madan, B.; Sharp, K. A. Changes in water structure induced by a hydrophobic solute proved by simulation of the water hydrogen bond angle and radial distribution functions. *Biophys. Chem.* **1999**, *78*, 33−41.

(27) Madan, B.; Sharp, K. A. Hydration Heat Capacity of Nucleic Acid Constituents Determined from the Random Network Model. *Biophys. J.* **2001**, *81*, 1881−1887.

(28) Sharp, K. A.; Madan, B. Hydrophobic Effect, Water Structure, and Heat Capacity Changes. *J. Phys. Chem. B* **1997**, *101*, 4343−4348.

(29) Sharp, K. A.; Madan, B.; Manas, E.; Vanderkooi, J. M. Water structure changes induced by hydrophobic and polar solutes revealed by simulations and infrared spectroscopy. *J. Chem. Phys.* **2001**, *114* (4), 1791−1796.

(30) Vanzi, F.; Madan, B.; Sharp, K. Effect of the Protein Denaturants Urea and Guanidinium on Water Structure: A Structural and Thermodynamic Study. *J. Am. Chem. Soc.* **1998**, *120*, 10748−10753.

(31) Yang, C.; Sharp, K. A. The mechanism of the type III antifreeze protein action: a computational study. *Biophys. Chem.* **2004**, *109*, 137−148.

(32) Woutersen, S.; Emmerichs, U.; Nienhuys, H.-K.; Bakker, H. J. Anomalous Temperature Dependence of Vibrational Lifetimes in Water and Ice. *Phys. Rev. Lett.* **1998**, *81* (5), 1106−1109.

(33) Jeffrey, G. A. *An Introduction to Hydrogen Bonding*; Oxford University Press: New York, 1997.

(34) Scheiner, S.; Cuma, M. Relative Stability of Hydrogen and Deuterium Bonds. *J. Am. Chem. Soc.* **1996**, *118*, 1511−1521.

(35) Schulz, P. C. DSC analysis of the state of water in surfactant-based microstructures. *J. Therm. Anal. Calorim.* **1998**, *51* (1), 135−149.

(36) Douzou, P. *Cryobiochemistry*: *An Introduction*; Academic Press: London, 1977.

(37) Babu, C. R.; Hilser, V. J.; Wand, A. J. Direct access to the cooperative substructure of protein and the protein ensemble via cold denaturation. *Nat. Struct. Mol. Biol.* **2004**, *11* (4), 352−357.

(38) Munson, C. A.; Baker, G. A.; Baker, S. N.; Bright, F. V. Effects of Subzero Temperatures on Fluorescent Probes Sequestered withing Aerosol-OT Reverse Micelles. *Langmuir* **2004**, *20*, 1551−1557.

(39) Zelent, B.; Nucci, N. V.; Vanderkooi, J. M. Liquid and ice water and glycerol/water glasses compared by infrared spectroscopy from 295 to 12 K. *J. Phys. Chem.* **2004**, *108*, 11141−11150.

(40) Devlin, J. P.; Joyce, C.; Buch, V. Infrared Spectra and Structures of Large Water Clusters. *J. Phys. Chem. A* **2000**, *104*, 1974−1977.

(41) Devlin, J. P.; Sadlej, J.; Buch, V. Infrared Spectra of Large H_2O Clusters: New Understanding of the Elusive Bending Mode of Ice. *J. Phys. Chem. A* **2001**, *105*, 974−983.

(42) D'Aprano, A.; Lizzio, A.; Liveri, V. T. Enthalpies of Solution and Volumes of Water in Reversed AOT Micelles. *J. Phys. Chem.* **1987**, *91*, 4749−4751.

(43) Shen, X.; Gao, H.; Wang, X. What makes the solubilization of water in reversed micelles exothermic or endothermic? A titration calorimetry investigation. *Phys. Chem. Chem. Phys.* **1999**, *1*, 463−469.

(44) Mukherjee, K.; Moulik, S. P. Thermodynamics of Micellization of Aerosol OT in Polar and Nonpolar Solvents. A Calorimetric Study. *Langmuir* **1993**, *9*, 1727−1730.